Effects of Manufacturing Process in Crash Simulations

J. Šašek[a,*], M. Pašek[a], K. Beneš[a], V. Glac[a]

[a]*MECAS ESI, s. r. o., Brojova 16, 326 00 Plzeň, Czech Republic*

Abstract

This article describes an impact of a manufacturing, which can significantly change real parts behavior. The influence of technology process is neglected in regular simulations. However, advanced finite elements solvers make possible to involve the manufacturing process in final simulations. It brings distortions and initial distribution of stress and strain into simulations. The possibilities are demonstrated on a crash simulation of a simple box-beam, where stamping and welding processes and spring-back are considered. All mentioned operations are performed in Virtual Performance Solution. The effects of manufacturing process are discussed with a respect to common simulation practice at the end of the paper.
© 2010 University of West Bohemia. All rights reserved.

Keywords: spot welds, Multi Model Coupling, chaining of simulations, manufacturing effects, FEM, crash

1. Introduction

Nowadays, numerical simulations are essential for design and development of any industrial product. They significantly decrease time and financial costs necessary for the development. The main disadvantage of simulations is inaccuracy caused by neglections and simplifications. Hence, new methodologies for improving accuracy are being investigated. Involving manufacturing process into a simulation is one of them. The influence of stamping (strain and thinning) is studied for example on frontal car crash response in [5]. Our contribution demonstrates influence of the whole technology process on a simple boxbeam model, which represents car longeron in crash loading (see Fig. 1). All simulations are based on a finite element method and performed in Virtual Performance (VP) Solution (PAM-CRASH).
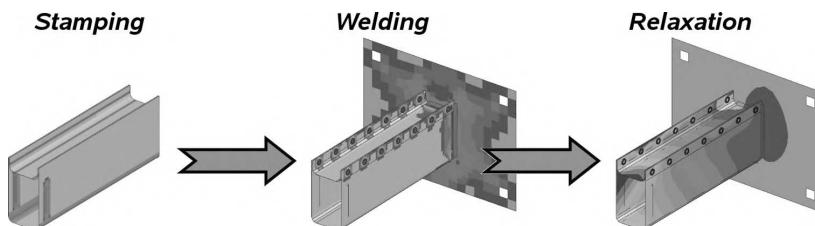

Fig. 1. Manufacturing process flow

---

*Corresponding author. Tel.: +420 377 432 931, e-mail: jakub.sasek@mecasesi.cz.

2. Stamping simulation

The influence of stamping effects, such as thinning and plastic deformation, is very important for correct prediction of structural colapse in buckling loading. Thus, stamping simulations are more and more used to predict those effects, especially in automotive industry. Classical stamping simulation, which needs exact CAD model of punch and die, can not be used effectively in the concept phase of the product. At this stage in one hand usually no precise CAD data of tools exist and on other hand creating of such a simulation is time consuming. That's why an alternative inverse simulation, where tools are not needed, starts to be used in current analysis. The classical stamping simulation shows better results but reasonable precision of stamping effects can be achieved on most industrial parts with an inverse approach. This brings finite element models much closer to the reality even in concept phase.

In stamping, which is the first stage, the lower and the upper sheets are formed by using inverse method [7]. The inverse simulation allows the user to calculate the initial blank from the finite element model of the stamped part, and to have information on the feasibility of the stamped part. The starting point of inverse simulation is the Finite Element model of the stamped part. The inverse algorithms find the position of the nodes of the blank in its original, horizontal or curved surface. A displacement field is thus associated to the stamping operation considered.
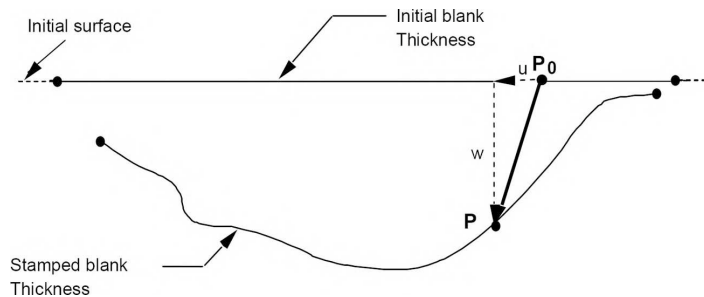

Fig. 2. Scheme of inverse stamping [7]

The formulation of the problem is summarized in the fig. 2, where P_0 represents position of a node belonging to initial blank and P is position of the corresponding node belonging to stamped blank. The characteristic feature of the inverse problem is that the unknowns are distributed between the initial blank (result of the computation) and the stamped part (starting point of the computation). The problem can be thus posed in mathematical terms: Find the displacements u and v so that, given a field of vertical displacement w, the stamped part is in equilibrium under the action of internal stresses, reaction forces, friction forces, and restraining forces. In order to find the solution, we must find the minimum of the total energy functional

$$\min_{u,v} \left(\Phi(\varepsilon_{ij}) + W(u_i) \right), \tag{1}$$

where Φ is internal strain energy and W is work of external forces.

Back to our application, the boxbeam is composed of two parts (upper and lower), which are welded together. Plastic strain and element's thickness of the both parts are displayed in the Fig. 3. The maximal plastic strain is equal to 0.079 in the case of upper part and 0.108 in the case of lower part. The maximal thinning of upper part is $3.835 \cdot 10^{-4}$ mm and the maximal
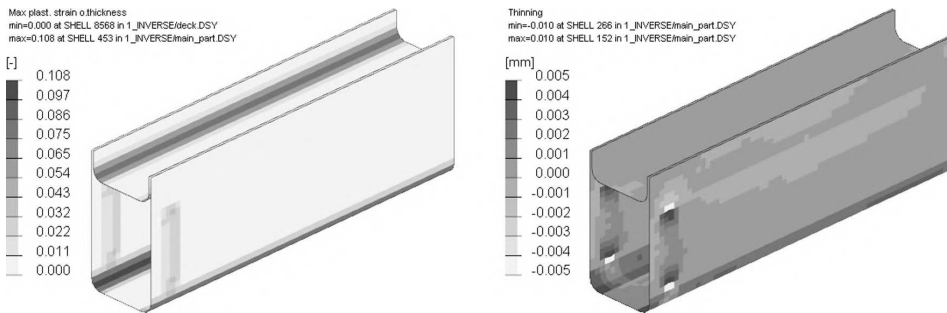
Fig. 3. Distribution of plastic strain (left side) and thinning (right side) after stamping simulation

thinning of lower part is $9.985 \cdot 10^{-3}$ mm. The results of the stamping simulation are stored in mapping files (see [9]), which will be used in the next simulation. It is not necessary to have topologically identical mesh, similar location of a mesh is sufficient in contradistinction to picking.

3. Welding simulation

Let's start with modelling of weld joints. The spot weld is relatively small area which is highly inhomogeneous in the term of material structure, see hardness distribution in the spot weld cut in the left side of Fig. 4. In explicit crash analysis we have limitation in element size because of the timestep. We need some simplification how to model these small inhomogeneous areas, so at present is the spot weld usually modelled by 1D or 3D macroelement. But these macroelements cannot satisfactorily describe crack propagation and energy absorption. That is the reason why we used detailed spot weld model, see right side of Fig. 4. In this model we can use advanced material models such as Johnson-Cook, Gurson or Wilkins (EWK) [4], which can predict failure and rupture. Timestep limitation for this detailed structure is solved by Multi Model Coupling [1, 2, 3] described in the following text.

For the detailed spot weld model, the ESI implementation of Wilkins rupture model (ESI-Wilkins-Kamoulakos) is used. Fracture occurs when the time integrated product of the equivalent plastic strain rate and two functions of the local stress distribution exceed a critical value
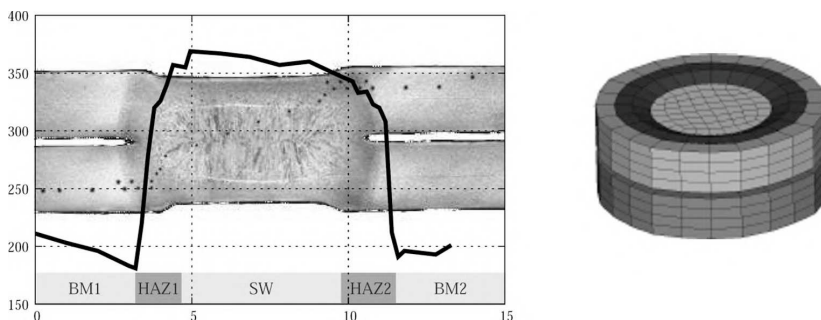

Fig. 4. Hardness distribution in the spotweld area (left side) [6] and fine mesh of the spotweld area with the heat-affected zone (right side)

D_c over a critical dimension R_c. The damage function is given by following equation

$$D = \int w_1 w_2 \, \mathrm{d}\bar{\varepsilon}^p. \tag{2}$$

The weighting parameter w_1 is related to the mean tensile stress and weighting parameter w_2 is related to the stress asymmetry. These parameters are given by

$$w_1 = \left(\frac{1}{1 + \frac{\sigma_m}{P_{lim}}} \right)^\alpha, \quad w_2 = (2 - A)^\beta, \tag{3}$$

where σ_m is hydrostatic stress, α, β are material constants, P_{lim} is theoretical material strength and $A = \max\left(S_2/S_3, S_2/S_1\right)$, where $S_1 \geq S_3 \geq S_3$ are mean component of deviator stress tensor. Material constants α and β can be determined by two ways. One is to performe set of experimental tests in tension and torsion with specimens with and without notch. After that computational simulations of these tests are performed to calibrate material models. Second possibility is to use automatic calibrator which is implemented directly in the solver. This way is widely used in case there is not enough tests and only standard tension test is available. The automatic calibrator was used in this case.

The simulation of welding is realized by using thermal analysis (thermal dilatation) in VP Implicit [9]. The material of spot welds and filled welds is locally heated on $1\,550\,^\circ\mathrm{C}$ at the beginning. The initial temperature of the rest of the material is $20\,^\circ\mathrm{C}$. The heated material (welds) is sequentially cooled according to technology of welding (see Fig. 5). Spot welds (1–14) are cooled at first, then filled welds (15–18) are cooled. A thermal dilatation (shrinkage) yields stress and strain, which causes initial stress and distortion to the boxbeam.
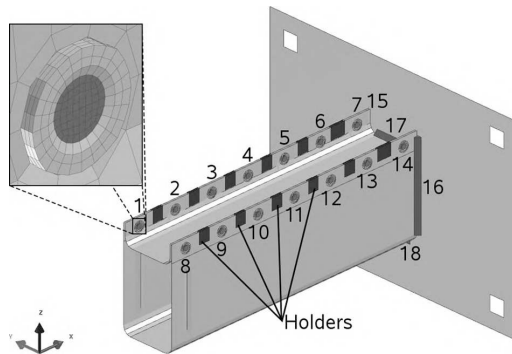

Fig. 5. Sequence of welding (cooling)

The spot welds are modelled by using fine solid mesh (see Fig. 5) according to real heterogeneity of spot welds. Fine solid mesh allows to consider spot weld geometry and heterogeneity of its material. This approach is also suitable for the spot welds rupture, which will be modelled in the crash section by element elimination. The filled welds are modelled by penta solid elements. The rest of structure is modelled by shell elements, which take initial stress and strain from previous stamping simulation. The technology of mapping is used in this case. The rear plate is fixed during cooling by boundary conditions. Holders (fixed in x direction) between spot welds are represented also via boundary conditions.

Results of welding simulation are displayed in Fig. 6. The maximal magnitude of displacement is 0.417 mm. The highest value of equivalent stress (1.532 GPa) is located near the filled welds (lower corners). Concerning spot welds, the maximum of solids is 1.318 GPa and the maximum of shells (surrouding area) is 1.265 GPa. Results of welding are used in the next simulation of relaxation after welding. A PICKING technology (see [10]) is used for the transfer of results from the welding simulation to the relaxation simulation. The PICKING means that the plastic strain and stress from the final state of the first simulation are transfered to the initial state of the next simulation in all integration points of coresponding elements.
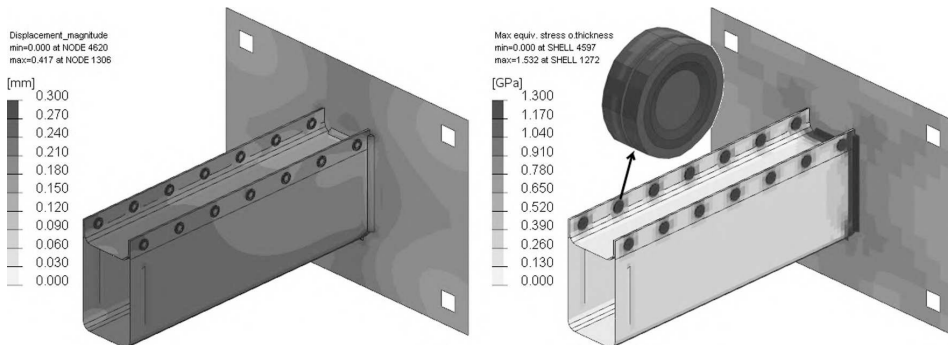

Fig. 6. Distribution of displacement magnitude (left side) and equivalent plastic stress (right side) after welding

4. Simulation of relaxation

The last presimulation represents relaxation after the welding. The implicit simulation computes nodal distortion after releasing holders. It is effective to use a SPRINGBACK option which releases the structure gradually (prevention of sudden unloading). Result of this process is the relaxed structure in equilibrium state which corresponds to deformed shape of the isolated part.

Results after relaxation are displayed in Fig. 7. The maximal magnitude of displacement is 0.118 mm (particularly in y-direction). The highest value of equivalent stress, located near the
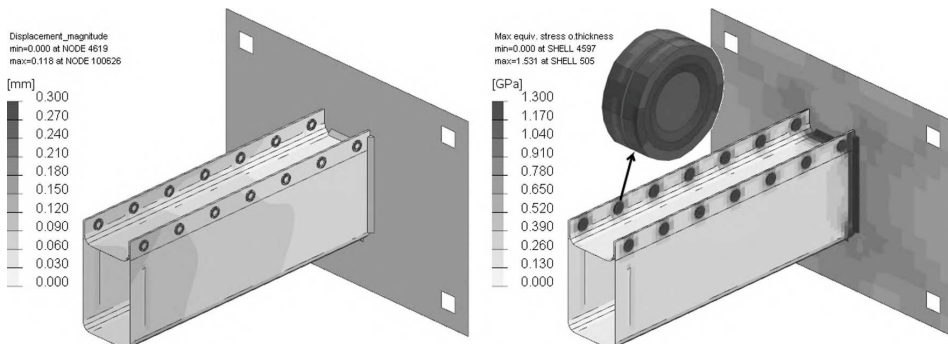

Fig. 7. Distribution of displacement magnitude (left side) and equivalent plastic stress (right side) after relaxation

filled welds, decreases to 1.531 GPA. The maximum of spot welds remains 1.318 GPA (solid elements). The final state (distorted nodes, plastic strain and stress) is picked in a crash simulation. The structure of the boxbeam is loaded by moving rigid plate which represents loading during frontal car crash. The motion of the rigid plate is imposed by constant acceleration.

5. Crash simulation

The crash simulation is performed by using Multi Model Coupling (MMC) [1] technology in VP Explicit [10] where the boxbeam is loaded by moving rigid wall. We can decrease dramatically computation time of the simulation by MMC approach and bring predictive rupture models to the daily use. The scheme of MMC is shown in Fig. 8.
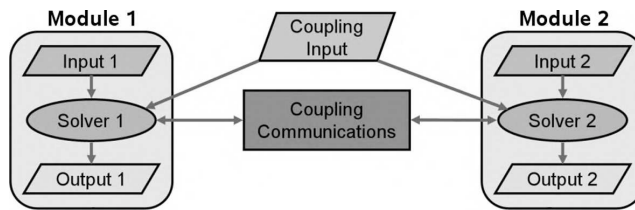

Fig. 8. Scheme of Multi Model Coupling

The model is divided into two standalone modules (domains). The connection between modules is performed by contact and tied elements. MMC allows to have domains with different timestep and thus speed-up the explicit simulation to reasonable CPU time in case of using more CPUs. The reduction of CPU time can be reached by appropriate choice of CPU number used for each module. The communication between domains is realized during a hyper-cycle which corresponds to a larger time step. We can express ratio of time steps as $R_{\Delta t} = \Delta t_1 / \Delta t_2$ where Δt_1 is time step of the first module and Δt_2 is time step of the second module.

Let's move on our model, the first domain (Module 1, $\Delta t_1 = 0.448$ ms) contains all entities except flanges with spot welds (see Fig. 9). Flanges with spot welds, which are modelled by solid elements, are involved in the second domain (Module 2, $\Delta t_2 = 0.044\,8$ ms). The rupture of spot welds is modelled by using element elimination with maximal plastic strain criterion.
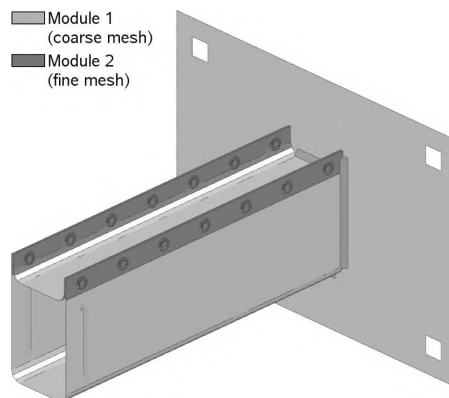

Fig. 9. MMC decomposition of the boxbeam (fine mesh – Module 1, coarse mesh – Module 2)

The first domain can have longer time step because of bigger elements (shells). This method increases a performance of simulation, because only one part is computed with small time step. The interface between domains is realized by contact and tied links (see [8]). Flanges are constrained by tied links to the rest of the boxbeam. The maximal time step ratio is limited to 10 in both examples (with and without presimulations). The elapsed time for the Multi Model Coupling run is about 14.5 hours. The MMC approach is about 4.7 times faster than classical one (elapsed time about 68 hours) where one model with small timestep is used.
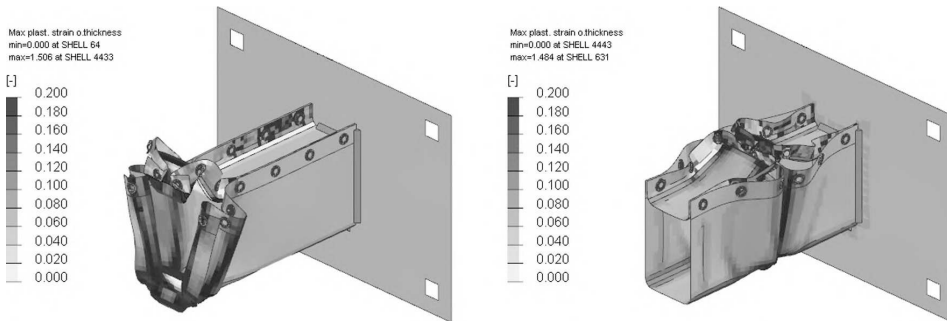

Fig. 10. Deformation mode without presimulations (left) and with presimulations (right)

The influence of presimulation is demonstrated in the Fig. 10. Deformation modes of the boxbeam without presimulations (left) and with presimulations (right) are compared there. Presimulations cause a change of deformation mode. The crashbox collapses in the middle in case of presimulations. Unlikely, the crashbox without presimulations breaks down in the front. This phenomenon is imposed by locally stiffened areas (initial plastic strain) and by the deflexion to the ideal perpendicular shape (see displacements after welding and relaxation).
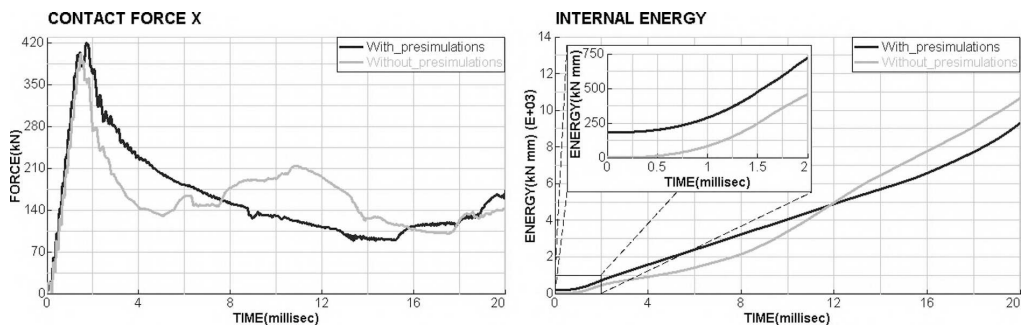

Fig. 11. The time history of contact force x and the time history of internal energy

Time history of contact force x and time history of internal energy are shown in Fig. 11. Presimulations decrease the buckling resistance of the boxbeam from 420.3 kN to 401.6 kN (4.45 %). The rest of the contact curve is also changed due to the deformation mode and the sequence of the spot weld fracture. Presimulations affect the time history of internal energy of the boxbeam. Initial deformations of presimulations are visible in the detailed view of internal energy – nonzero value at the beginning of curve. The final total internal energy of the boxbeam without presimulations is 10.75 kJ and the total internal energy of the boxbeam with presimulations is 9.40 kJ. The relative change is equal to 12.56 %.

6. Conclusion

The change of deformation mode demonstrates the sense and the influence of presimulations which bring initial plastic strain, stress and thinning. Areas with high plastic strain values cause local stiffening. Distortion of the boxbeam is given by thermal simulation (welding) and can strongly affect deformation mode of structure loaded in longitudinal direction (buckling). Presimulations can strongly affect the buckling resistance of the boxbeam and internal energy, which can be absorbed by the structure (see Fig. 11). This aspects are very important for structure assessing.

All simulations are performed in the Virtual Performance Solution (PAM-CRASH) which makes possible to engage all computations into manufacturing process. The methodology of presimulations improves accuracy and can be easily involved into simulations commonly used in wide range of applications, especially in automotive industry. MMC technology allows us to involve fine meshed parts into a simulation, what provides physically more faithful model (results) with acceptable CPU time.

References

[1] Greve, L., Vlachoutsis, S., Multi-scale and multi-model methods for efficient crash simulation, International Journal of Crashworthiness, Volume 12, Issue 4 (2007) 437–448.
[2] Vlachoutsis, S., Greve, L., Multi-Model Coupling for Crash Simulation: Methodology, Applications and Performance Investigation, Proceedings of the 15th European Conference EuroPAM 2005, Potsdam, ESI Group, 2005.
[3] Greve, L., Failure Modelling of Cast Aluminium and Industrial Application Using Multi-Model Coupling in PAM-CRASH, Proceedings of the 15th European Conference EuroPAM 2005, Potsdam, ESI Group, 2005.
[4] Kamoulakos, A., Predictive rupture simulation in manufacturing: an approach with the EWK model, Proceedings of the FLC'06 Conference, Zurich, ETH Zurich, 2006.
[5] Takashina, K., Ueda, K., Ohtsuka, T., Investigation of Accuracy Improvement on Crashworthiness Simulation with Pre-Simulation of Metal Forming, Proceedings of the 7th European LS-DYNA Conference, Salzburg, 2009.
[6] Seeger, F., Michel, G., Blanquet, M., Investigation of Spot Weld Behaviour Using Detailed Modeling Technique, 7. LS-DYNA Anwenderforum, Bamberg, 2008.
[7] Pam-Stamp 2G & Pam-Tube 2G, 2009. User's Guide. ESI Group.
[8] Virtual Performance Solution, 2009. Explicit Solver Reference Manual. ESI Group.
[9] Virtual Performance Solution, 2009. Implicit Solver Reference Manual. ESI Group.
[10] Virtual Performance Solution, 2009. Solver Notes Manual. ESI Group.